

Zero absorption and large negative refractive index in a left-handed four-level atomic media

ShunCai Zhao ^{1, 2, 3, *} ZhengDong Liu,^{1, 2, 3, †} and Qixuan Wu⁴

¹*School of Materials Science and Engineering, Nanchang University, Nanchang 330031, PR China*

²*Engineering Research Center for Nanotechnology, Nanchang University, Nanchang 330047, PR China*

³*Institute of Modern Physics, Nanchang University, Nanchang 330031, PR China*

⁴*English department, Hainan University, Danzhou 571737, PR China*

In this paper, we have investigated three external fields interacting with the four-level atomic system described by the density-matrix approach. The atomic system exhibits left-handedness with zero absorption as well as large negative refractive index. Varying the parameters of the three external fields, the properties of zero absorption, large negative refractive index from the atomic system keep unvarying. Our scheme proposes an approach to obtain negative refractive medium with zero absorption. The zero absorption property of atomic system may be used to amplify the evanescent waves that have been lost in the imaging by traditional lenses. And a slab fabricated by the left-handed atomic system may be an ideal candidate for designing perfect lenses.

INTRODUCTION

The propagation of electromagnetic waves in matter is characterized by the frequency-dependent relative dielectric permittivity ϵ_r and magnetic permeability μ_r . And their product defines the index of refraction: $\epsilon_r \cdot \mu_r = n^2$. The left-handed material(LHM) has a negative refractive index with the permittivity and permeability being negative simultaneously[1]. And there're much remarkable progress demonstrates negative refractive index using technologies such as artificial composite metamaterials [2-14], transmission line simulation[15], photonic crystal structures[16-21] and photonic resonant materials [22-26]. The former three methods, based on the classical electromagnetic theory, require delicate manufacturing of spatially periodic structure. The last method is a quantum optical approach where the physical mechanism is the quantum interference and coherence that arises from the transition process in a multilevel atomic system. The LHM becomes a very active area of research because of one of the goals of "perfect lens" in which imaging resolution is not limited by the wavelength [27]. However, the results in Ref.[28-29]show that the LHM lenses can indeed amplify the evanescent waves that have been lost in the imaging by traditional lenses,the presence of absorption(even a small amount) plays a crucial rule in recovery of the lost evanescent waves,thereby controlling the quality of imaging,and makes LHM lenses less perfect. So, the key challenge remains the realization of negative refraction without absorption, which is particularly important in the optical regime[30-32].

With the realization of negative refractive index without absorption in mind, here we propose a promising new approach: the use of quantum interference effects causing electromagnetically induced transparency(EIT)[33]to realize left-handedness with zero absorption. Under some appropriate conditions,the system shows negative values for permittivity and permeability simultaneously , zero absorption as well as a large negative refractive index.Our approach for left-handedness without absorption is different from Ref.[34]and our scheme allows us to engineer the value of the refractive index while maintaining vanishing absorption[35] to the beam.In this sense, our approach implements modifying the optical response of an atomic medium.

The paper is organized as follows.In Section 2, we present our model and its expressions for the electric permittivity,magnetic permeability and refractive index.In Section 3, we present numerical results and their discussion. This is followed by concluding remarks in Section 4.

THEORETICAL MODEL

Consider a four-level atomic ensemble interacting with three optical fields, i.e. the coupling beam,probe light and signal field. The configuration of such a four-level system is depicted in Fig.1. The coupling field E_c (frequency ω_c) is acting on the transition $|3\rangle$ and $|4\rangle$ (with transition frequency ω_{34}).The weak probe field E_p (frequency ω_p)interacts with the transition $|2\rangle$ to $|3\rangle$ (transition frequency ω_{23}),and its electric and magnetic fields are coupled to the level pairs $|3\rangle$ - $|2\rangle$ and $|2\rangle$ - $|1\rangle$, respectively. While the weak signal field E_s (frequency ω_s)drives the transition $|1\rangle$ to $|3\rangle$ (transition frequency ω_{13}). The frequency detunings of these three optical fields are Δ_c, Δ_p and Δ_s , respectively. The Rabi frequencies of these optical fields are denoted by Ω_c, Ω_p and Ω_s , respectively. All the Rabi frequencies are assumed to be real. We consider the two levels, $|3\rangle$ and $|2\rangle$ have opposite parity with $d_{23} = \langle 2|\vec{d}|3\rangle \neq 0$, and \vec{d} is the electric dipole operator. The levels $|2\rangle$ and $|1\rangle$ have the same parity, $\mu_{12} = \langle 1|\vec{\mu}|2\rangle \neq 0$, where the $\vec{\mu}$ is the magnetic dipole operator. The radiative decay constants from levels $|4\rangle$ to $|3\rangle$, $|3\rangle$ to $|2\rangle$ and $|3\rangle$ to $|1\rangle$ are $\gamma_4, \gamma_2, \gamma_3$. γ_1 is related to non-radiative relaxation of state $|2\rangle$.Under the condition that lower levels are equally populated and the decay rate of level $|1\rangle$ is quite small, then levels $|1\rangle, |3\rangle$ and $|4\rangle$ are in a three-level ladder-type configuration and level $|2\rangle$, together with levels $|3\rangle$ and $|4\rangle$ forms another three-level ladder-type configuration.

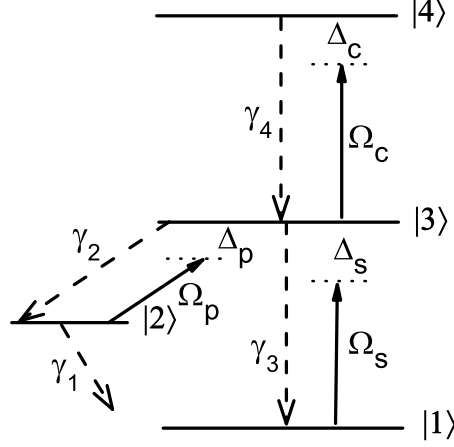


FIG. 1. Schematic diagram of a four-level atomic system interacting with three electromagnetic fields, Ω_c , Ω_p and Ω_s . The level pairs $|2\rangle$ - $|3\rangle$ and $|2\rangle$ - $|1\rangle$ are coupled to the electric and magnetic fields of Ω_p (the weak probe light), respectively.

For this system the Hamiltonian under the dipole and rotating-wave approximation (RWA) can be written as,

$$\hat{H} = \Delta_p|2\rangle\langle 2| + \Delta_s|1\rangle\langle 1| + \Delta_c|4\rangle\langle 4| + [\Omega_p|3\rangle\langle 2| + \Omega_s|3\rangle\langle 1| + \Omega_c|3\rangle\langle 4| + H.c.] \quad (1)$$

Using the density-matrix approach, the time-evolution of the system is described as

$$\frac{d\rho}{dt} = -\frac{i}{\hbar}[H, \rho] + \Lambda\rho, \quad (2)$$

In which $\Lambda\rho$ represents the irreversible decay part in the system which is a phenomenological added decay term that corresponds to the incoherent processes. And the density-matrix equations of motion in the dipole and RWA for this system can be written as follows,

$$\rho_{11}^{\dot{}} = 2\gamma_3\rho_{33} + 2\gamma_1\rho_{22} + i\Omega_s(\rho_{13} - \rho_{31}) \quad (3)$$

$$\rho_{22}^{\dot{}} = 2\gamma_2\rho_{33} - 2\gamma_1\rho_{22} + i\Omega_p(\rho_{23} - \rho_{32}) \quad (4)$$

$$\rho_{33}^{\dot{}} = -2(\gamma_2 + \gamma_3)\rho_{33} + 2\gamma_4\rho_{44} - i\Omega_s(\rho_{13} - \rho_{31}) - i\Omega_p(\rho_{23} - \rho_{32}) + i\Omega_c(\rho_{34} - \rho_{43}) \quad (5)$$

$$\rho_{44}^{\dot{}} = -2\gamma_4\rho_{44} - i\Omega_c(\rho_{34} - \rho_{43}) \quad (6)$$

$$\rho_{12}^{\dot{}} = -[\gamma_1 - i(\Delta_s - \Delta_p)]\rho_{12} + i\Omega_p\rho_{13} - i\Omega_s\rho_{32} \quad (7)$$

$$\rho_{13}^{\dot{}} = -(\gamma_2 + \gamma_3 - i\Delta_s)\rho_{13} + i\Omega_p\rho_{12} + i\Omega_c\rho_{14} + i\Omega_s(\rho_{11} - \rho_{33}) \quad (8)$$

$$\rho_{14}^{\dot{}} = -[\gamma_4 - i(\Delta_s + \Delta_c)]\rho_{14} + i\Omega_c\rho_{13} - i\Omega_s\rho_{34} \quad (9)$$

$$\dot{\rho}_{23} = -(\gamma_2 + \gamma_3 - i\Delta_p)\rho_{23} + i\Omega_s\rho_{21} + i\Omega_c\rho_{24} + i\Omega_p(\rho_{22} - \rho_{33}) \quad (10)$$

$$\dot{\rho}_{24} = -[\gamma_1 + \gamma_4 - i(\Delta_p + \Delta_c)]\rho_{24} + i\Omega_c\rho_{23} - i\Omega_p\rho_{34} \quad (11)$$

$$\dot{\rho}_{34} = -(\gamma_2 + \gamma_3 + \gamma_4 - i\Delta_c)\rho_{34} - i\Omega_s\rho_{14} - i\Omega_p\rho_{24} + i\Omega_c(\rho_{33} - \rho_{44}) \quad (12)$$

Where the frequency detunings of these three optical fields are $\Delta_c = \omega_c - \omega_{34}$, $\Delta_p = \omega_p - \omega_{23}$ and $\Delta_s = \omega_s - \omega_{13}$, respectively.

In the following, we will discuss the electric and magnetic responses of the medium to the probe field. It should be noted that here the atoms are assumed to be nearly stationary (e.g., at a low temperature) and hence any Doppler shift is neglected. When discussing how the detailed properties of the atomic transitions between the levels are related to the electric and magnetic susceptibilities, one must make a distinction between macroscopic fields and the microscopic local fields acting upon the atoms in the vapor. In a dilute vapor, there is little difference between the macroscopic fields and the local fields that act on any atoms (molecules or group of molecules) [36]. But in dense media with closely packed atoms (molecules), the polarization of neighboring atoms (molecules) gives rise to an internal field at any given atom in addition to the average macroscopic field, so that the total fields at the atom are different from the macroscopic fields [36]. In order to achieve the negative permittivity and permeability, here the chosen vapor with atomic concentration $N = 5 \times 10^{24} m^{-3}$ should be dense, so that one should consider the local field effect, which results from the dipole-dipole interaction between neighboring atoms. In what follows we first obtain the atomic electric and magnetic polarization, and then consider the local field correction to the electric and magnetic susceptibilities (and hence to the permittivity and permeability) of the coherent vapor medium. With the formula of the atomic electric polarizations $\gamma_e = 2d_{23}\rho_{23}/\epsilon_0 E_p$, where $E_p = \hbar\Omega_p/d_{23}$ one can arrive at

$$\gamma_e = \frac{2d_{23}^2\rho_{32}}{\epsilon_0\hbar\Omega_p} \quad (13)$$

In the similar fashion, by using the formulae of the atomic magnetic polarizations $\gamma_m = 2\mu_0\mu_{12}\rho_{21}/B_p$ [36], and the relation of between the microscopic local electric and magnetic fields $E_p/B_p = c$ we can obtain the explicit expression for the atomic magnetic polarizability. Where μ_0 is the permeability of vacuum, c is the speed of light in vacuum. Then, we have obtained the microscopic physical quantities γ_e and γ_m . In order to achieve a significant magnetic response, the transition frequency between levels $|2\rangle$ - $|3\rangle$, and $|2\rangle$ - $|1\rangle$ should be approximately equal to the frequency of the probe light. Thus, the coherence ρ_{12} drives a magnetic dipole, while the coherence ρ_{23} drives an electric dipole. However, what we are interested in is the macroscopic physical quantities such as the electric and magnetic susceptibilities which are the electric permittivity and magnetic permeability. The electric and magnetic Clausius-Mossotti relations can reveal the connection between the macroscopic and microscopic quantities. According to the Clausius-Mossotti relation [36], one can obtain the electric susceptibility of the atomic vapor medium

$$\chi_e = N\gamma_e \cdot \left(1 - \frac{N\gamma_e}{3}\right)^{-1} \quad (14)$$

The relative electric permittivity of the atomic medium reads $\epsilon_r = 1 + \chi_e$. In the meanwhile, the magnetic Clausius-Mossotti [37]

$$\gamma_m = \frac{1}{N} \left(\frac{\mu_r - 1}{\frac{2}{3} + \frac{\mu_r}{3}} \right) \quad (15)$$

shows the connection between the macroscopic magnetic permeability μ_r and the microscopic magnetic polarizations γ_m . It follows that the relative magnetic permeability of the atomic vapor medium is

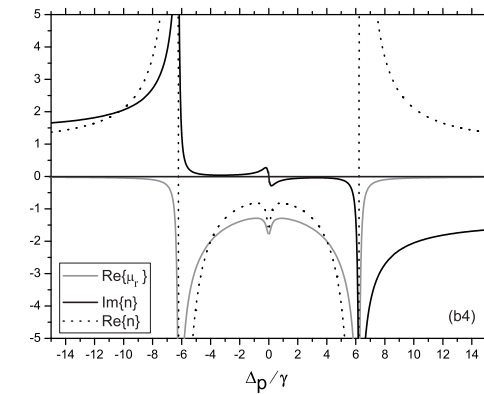
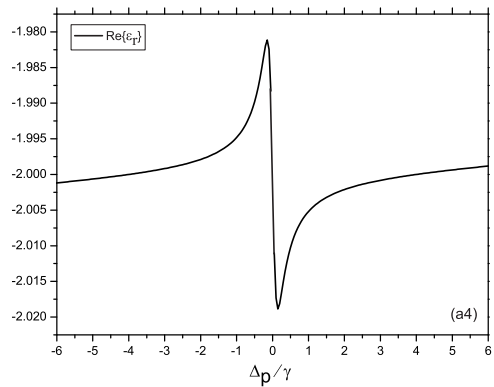
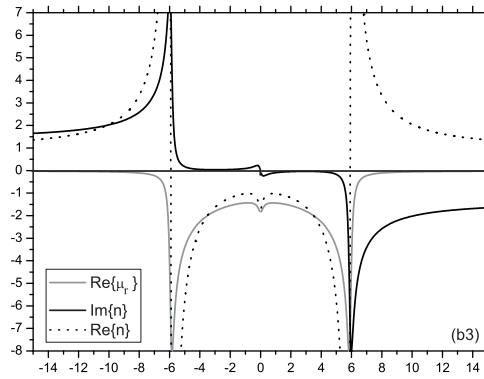
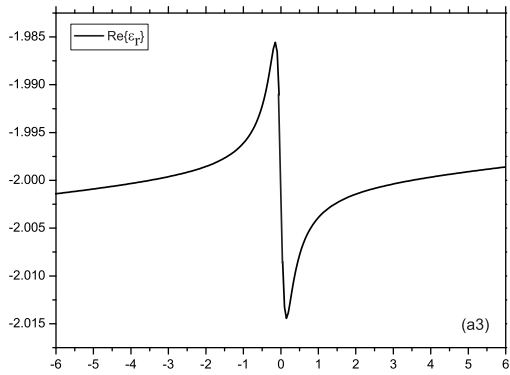
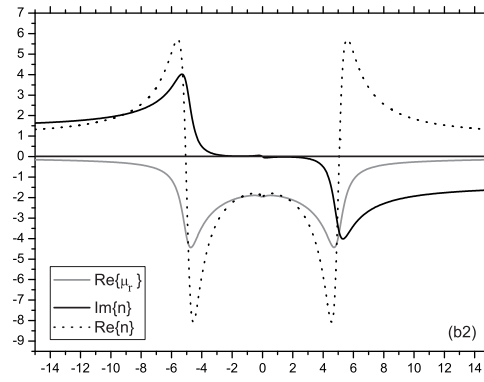
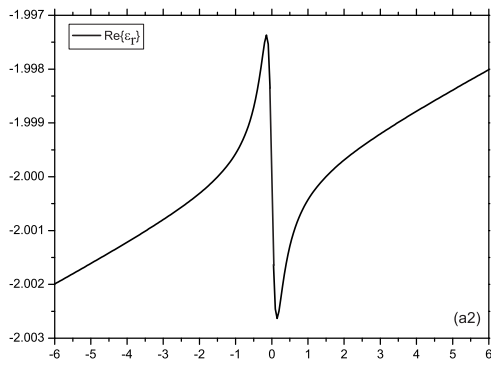
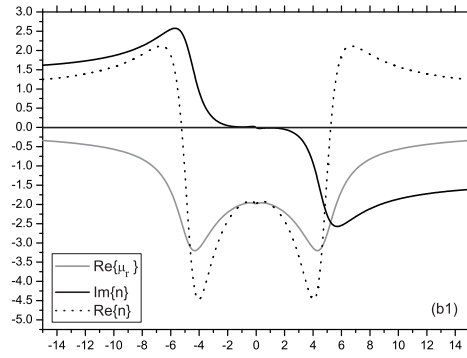
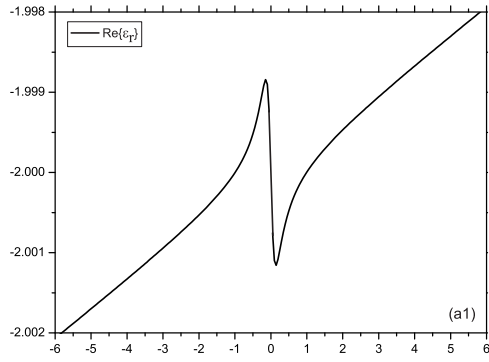
$$\mu_r = \frac{1 + \frac{2}{3}N\gamma_m}{1 - \frac{1}{3}N\gamma_m} \quad (16)$$

Substituting the expressions of ε_r and μ_r into $n = -\sqrt{\varepsilon_r\mu_r}$ [1], we can get the refractive index of left-handed materials. In the above, we obtained the expressions for the electric permittivity, magnetic permeability and refractive index of the four-level atomic medium. In the section that follows, we will get solutions to the density-matrix equations (3)-(11) under the steady-state condition.

RESULTS AND DISCUSSION

We firstly consider the coupling laser beam and signal laser beam are assumed to be on resonance simultaneously, and the atomic vapor medium with $N = 5 \times 10^{24}m^{-3}$ to examine the case of dense gas for the four level atom configuration. As pointed out in the following numerical example, the magnitude of the applied coherent optical field's Rabi frequency is ($10^8/s$), which is larger than the radiative decay constants. Thus, the effects of dephasing, and collisional broadening can be neglected, and the coherence effect can be maintained even increased in the atomic vapor under consideration. With the steady solution of the matrix equations(3)-(11) we can obtain the coherent terms ρ_{32} and ρ_{21} , and with the expressions for the atomic electric and magnetic polarizability (13)-(16) we will present a numerical example to show that the strong electric and magnetic responses can truly arise in the four-level coherent vapor medium under certain conditions. The strong electric and magnetic responses can lead to simultaneously negative permittivity and permeability at a certain wide frequency bands of the probe light. The real parts of the relative permittivity and permeability, refractive index are plotted in Figure 2, Figure 3 and Figure 4. We examine the left-handedness of the four-level atomic vapor. Largely, we concerned about the absorption behaviors and the values of the negative refractive index in the zero absorption intervals.

In Figure 2, we set the coupling field and signal field being resonant simultaneously, i.e., $\Delta_c = \Delta_s = 0$. Other parameters are scaled by $\gamma = 10^8/s$: $\gamma_1 = 0.05\gamma$, $\gamma_2 = \gamma_3 = 0.01\gamma$, $\gamma_4 = 0.1\gamma$, $\Omega_p = \Omega_s = 0.1\gamma$. $Re[\varepsilon_r]$ is plotted in Figure 2(a1) \rightarrow (a4), $Re[\mu_r]$ and the refractive index n are plotted in Figure 2(b1) \rightarrow (b4) versus the probe detuning Δ_p/γ with the Rabi frequency $\Omega_c = 1.0\gamma$, 1.5γ , 3.5γ , 4.0γ . And the solid, gray and dotted curves represent $Im[n]$, $Re[\mu_r]$ and $Re[n]$ in Figure 2(b1) \rightarrow (b4), respectively. It can be seen from Figure 2(a1) \rightarrow (a4) that the real parts of the relative dielectric permittivity keep negative values unchanged while varying the couple Rabi frequency. And the profiles are symmetry at the exact resonant location. The values of $Re[\mu_r]$ (gray curves in Figure 2(b1) \rightarrow (b4)) are negative too. Thus, the atomic system displays left-handedness with simultaneous negative permittivity and permeability. The absorption behaviors of the four-level atomic system are depicted by the imaginary part (the solid curve in Figure 2(b1) \rightarrow (b4)) of refractive index n . From the profile of the solid curves, we can see the zero absorption intervals widening with the variation of the couple field. And the intervals are about $[-2\gamma, 2\gamma]$ (in Figure 2(b1)), $[-3\gamma, 3\gamma]$ (in Figure 2(b2)). When the Rabi frequency $\Omega_c = 3.5\gamma$, the zero absorption interval is split into two: $[-4.6\gamma, -1\gamma]$ and $[1\gamma, 4.6\gamma]$ (in Fig. 2(b3)), approximately. In Figure 2(b4), the zero absorption intervals are $[-4.6\gamma, -1.8\gamma]$ and $[1.8\gamma, 4.6\gamma]$, which are narrow compared with those in Figure 2(b3). The dotted curves indicate that the real part of refractive index have negative values. And the maximums of $Re[n] \approx -2.5$ (in (b1)), ≈ -3 (in (b2)), ≈ -4 (in (b3)) and ≈ -2.8 (in (b4)) in the zero absorption intervals. The results indicate that the negative refractive index increase with the intensities of the control field, but high intensity may reduce the values while keeping zero absorption property unchanged. In the proof-of-principle experiment to enhance imaging resolution made by N.A. Proite et al. [35], the maximum refractive



index of an atomic vapor can reach to 2 approximately while keeping without absorption. Here we achieve zero absorption in the negative refractive index media, which maybe a possibility to overcome the defect mentioned in Ref.[28-29] and to enhance the resolution of image.

Figure 3 gives the absorption behaviors and the left-handedness when the coupling and signal fields are simultaneous off-resonant, i.e., the frequency detunings $\Delta_c = -1.5\gamma$, $\Delta_s = 1.5\gamma$. In Figure 3(c1) \rightarrow (c3), $Re[\epsilon_r]$ is plotted corresponding to the different Rabi frequencies (Ω_c): 1.0γ , 1.5γ , 3.5γ . We can see the negative values of $Re[\epsilon_r]$ and the unsymmetrical character of the profiles. The values of the real part of relative permeability depicted by gray curves are negative in Figure 3(b1) \rightarrow (b4). The atomic system still displays left-handedness when the signal and coupling fields are simultaneous off-resonant. We notice that the values of the imaginary part of the refractive index (depicted by the solid curves in Figure 3(d1) \rightarrow (d3)) are zero in the intervals of $[-2.5\gamma, 3.0\gamma]$ (in (d1)), $[-3.0\gamma, 3.5\gamma]$ (in (d2)) and $[-9.0\gamma, 11.2\gamma]$ (in (d3)). The zero absorption intervals are wider than those under the condition of the coupling field and signal field being resonant simultaneously in Figure 2. And the couple field is stronger, the zero absorption intervals are wider. The wide zero absorption intervals may provide the possibility to facilitate making "perfect" images. And the maximum values of negative refractive index are about -2.2 in (d1), -2.5 in (d2), -6 in (d3) in the zero absorption intervals. An effective positive refractive index of the designing three-dimensional isotropic metamaterials [38] reaches between 5.5 and 7 made by J. W. Shin et al.. Here we get a counter-intuitive negative values of the refractive index with zero absorption and the maximum negative value is -6, approximately.

In Figure 4, the signal field is set off-resonant (e.g., $\Delta_s = 1.5\gamma$) with the parameter value: $\Omega_c = 3.5\gamma$. We discuss the characteristics of absorption and the refractive index by varying the the probe field's Rabi frequencies ($\Omega_p = \Omega_s$) with 0.1γ , 1.0γ , 2.8γ . Other parameters are the same as those in Figure 2. The profiles of $Re[\epsilon_r]$ in (e1) \rightarrow (e3) and $Re[\mu_r]$ in (f1) \rightarrow (f3) display negative values. The simultaneous negative permittivity and permeability indicates the left-handedness of the atomic vapor medium. In (f1), the zero absorption intervals in the solid curves are about $[-3.6\gamma, 0]$ and $[2.3\gamma, 5\gamma]$ when the $\Omega_p = 0.1\gamma$. The zero absorption intervals are $[-5.2\gamma, 14\gamma]$ and $[-5.5\gamma, 14\gamma]$ when the $\Omega_p = 1.0\gamma, 2.8\gamma$ in (f2) and (f3). The maximum of $Re[n]$ in the zero absorption intervals are about -3.2, -3, -2.4 in (f1) \rightarrow (f3). Adjusting the intensity of probe beam properly, the zero absorption characteristics of the left-handed material atomic system can be manipulated with large flexibility.

CONCLUSION

In conclusion, we investigate three external fields interacting with the four-level atomic system. Under the condition of coupling and signal field being resonant simultaneously, the intensity of couple field can expand the zero absorption interval but high intensity may decrease the zero absorption ranges and negative refractive index of the medium. When the two light fields are off-resonant, the intensity of coupling field and the probe beam can also make no absorption in a wider interval with a large negative refractive index. The zero absorption property may be used to amplify the evanescent waves that have been lost in the imaging by traditional lenses. Our scheme proposes an approach to obtain negative refractive medium with zero absorption and the possibility to enhance the imaging resolution in realizing "superlenses". In our scheme, we can alter the value of the refractive index while maintaining vanishing absorption to the beam. In this sense, our approach implements modifying the optical response of an atomic medium.

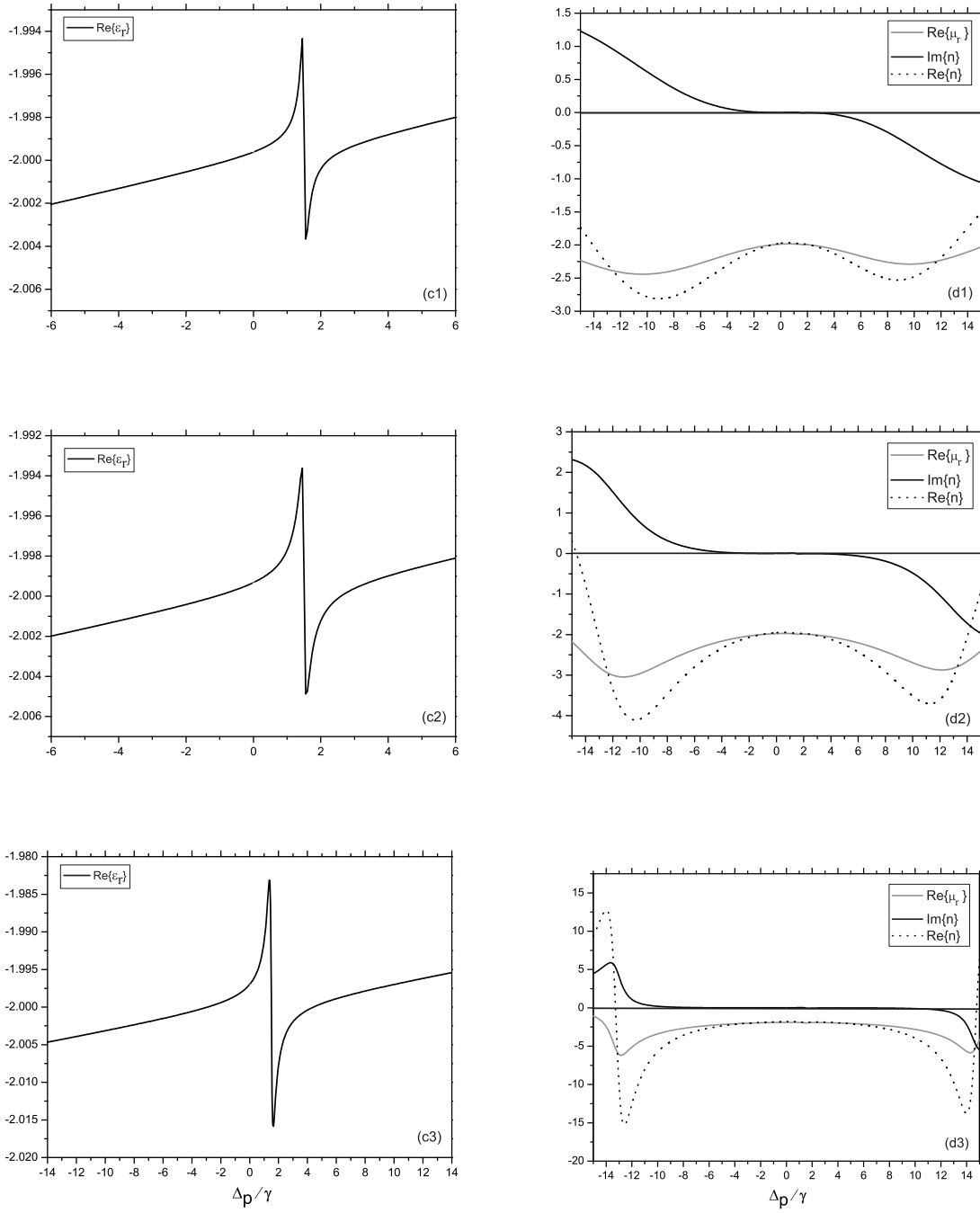


FIG. 3. Real parts of the permittivity and permeability, the refractive index as a function of $\Delta p/\gamma$ with: $\Delta_c = -1.5\gamma$, $\Delta_s = 1.5\gamma$, $\Omega_p = \Omega_s = 0.8\gamma$, $\Omega_c = 1.0\gamma, 1.5\gamma, 3.5\gamma$. Other parameters are the same as those in Figure 2.

ACKNOWLEDGMENTS

The work is supported by the National Natural Science Foundation of China (Grant No.60768001 and No.10464002).

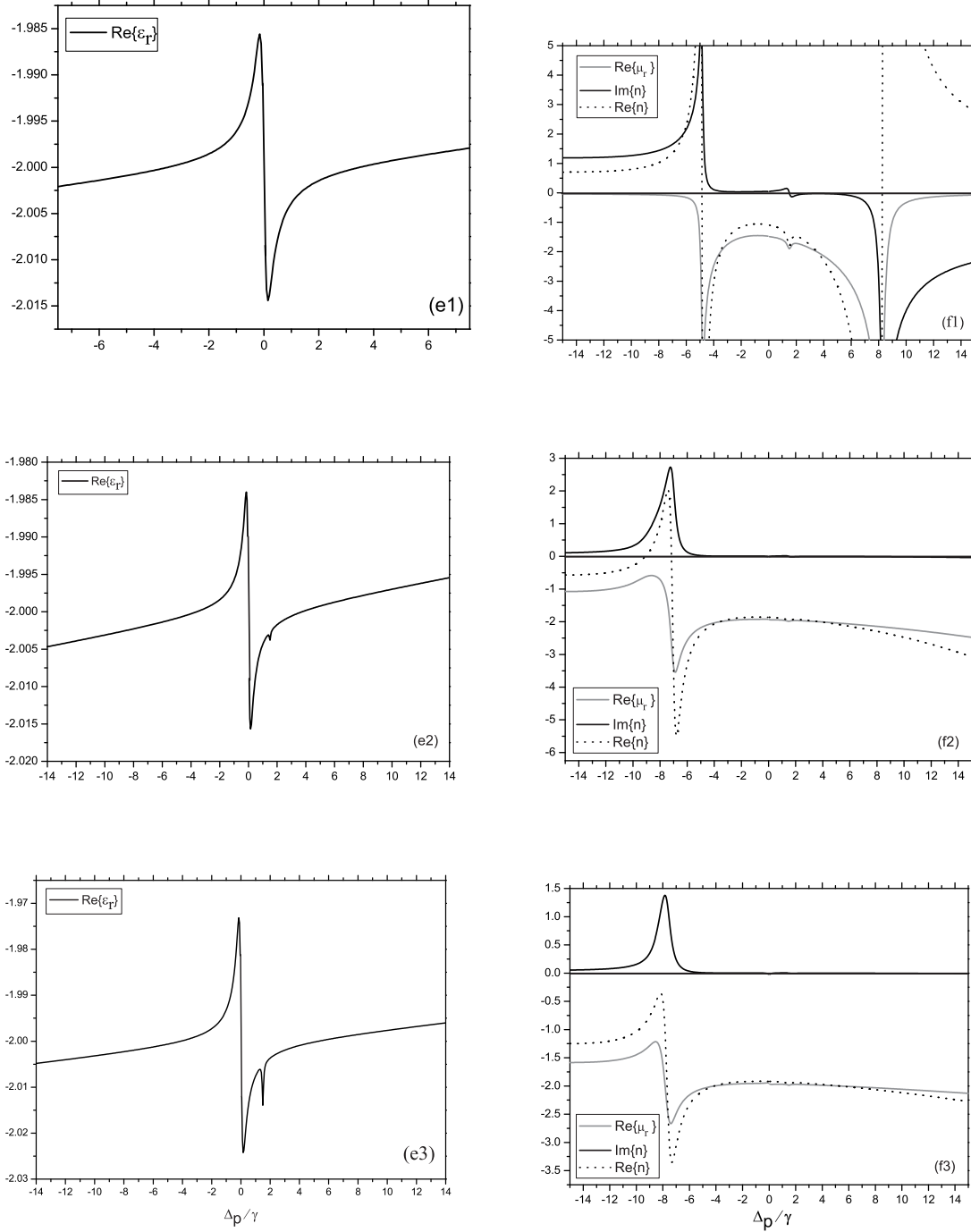


FIG. 4. Real parts of the permittivity and permeability, the refractive index as a function of $\Delta p/\gamma$ with: $\Omega_p = \Omega_s = 0.1\gamma, 1.0\gamma, 2.8\gamma, \Omega_c = 3.5\gamma, \Delta_s = 1.5\gamma$. Other parameters are the same as those in Fig. 2.

* Corresponding author zscnum1@126.com

† Corresponding author lzdgroup@ncu.edu.cn

- [1] V.G.Veselago 1968 *Sov.Phys.Usp.* **10** 509.
- [2] J.B.Pendry,A.J.Holden,D.J.Robbins,W.J.Stewart 1998 *Phys.Condens.Matter* **10** 4785.
- [3] J.B.Pendry,A.J.Holden,W.J.Stewart,I.Youngs 1996 *Phys.Rev.Lett.* **76** 4773.
- [4] V.Yannopapas,A. Moroz 2005 *J.Phys.:Condens. Matter* **17** 3717.
- [5] M.S. Wheeler,J.S. Aitchison,M.Mojahedi 2005 *Phys. Rev.B* **72** 193103.
- [6] J.B.Pendry et al. 1999 *IEEE Trans.Microwave Theory Tech.* **47** 2075.
- [7] D.R.Smith et al. 2000 *Phys.Rev.Lett.* **84** 4184.
- [8] R.Shelby,D.R.Smith, S.Schultz 2001 *Science* **77** 292.
- [9] T.J.Yen et al. 2004 *Science* **303** 1494.
- [10] S.Linden et al. 2004 *Science* **306** 1351.
- [11] C.Enkrich et al. 2005 *Phys.Rev.Lett.* **95** 203901.
- [12] J.B. Pendry 2004 *Science* **306** 1353.
- [13] V.Yannopapas 2006 *J. Phys.: Condens.Matter* **18** 6883.
- [14] S.Tretyakov,et al. 2005 *Photon. Nanostruct.* **3** 107.
- [15] G.V.Eleftheriades,A.K. Iyer,P.C.Kremer 2004 *IEEE Trans.Microwave Theory Tech.* **50** 2702.
- [16] S.He, Z.C.Ruan, L.Chen, J.Q.Shen 2004 *Phys. Rev. B* **70** 115113.
- [17] A.Berrier,M.Mulot,M.Swillo,M.Qiu,L.Thyl"n,A.Talneau,S.Anand 2004 *Phys.Rev.Lett.* **93** 073902.
- [18] Q.Thommen, P.Mandel 2006 *Opt. Lett.* **31** 1803.
- [19] P.V.Parimi et al. 2004 *Phys.Rev.Lett.* **92** 127401.
- [20] A.Berrier et al. 2004 *Phys.Rev.Lett.* **93** 073902.
- [21] Z.Lu et al. 2005 *Phys.Rev.Lett.* **95** 153901.
- [22] J.Q. Shen 2006 *Phys.Lett.A* **357** 54.
- [23] M.Ö.Oktel, Ö.E.M⁻¹stecapliouglu 2004 *Phys.Rev.A* **70** 053806.
- [24] Zh.G.Dong,Sh.Y. Lei, M.X. Xu,et al. 2008 *Phys.Rev.E* **77** 056609.
- [25] Q.Thommen, P.Mandel 2006 *Phys.Rev.Lett.* **96** 053601.
- [26] C.S. Zhao and D.Z. Liu 2009 *Int.J.Quant.Inf.* **7** 747.
- [27] J. B.Pendry 2000 *Phys.Rev.Lett.* **85** 3966.
- [28] N.Garcia,M.Nieto-Vesperinas 2002 *Phys.Rev.Lett.* **88** 207403.
- [29] Zhen Ye 2003 *Phys.Rev.B* **67** 193106.
- [30] V.M.Shalaev 2007 *Nature Photon*(London) **1** 41.
- [31] V.P.Drachev et al. 2006 *Laser Phys.Lett.* **3** 49.
- [32] G.Dolling,M.Wegener et al. 2007 *Opt.lett.* **32** 53.
- [33] M.Fleischhauer, A.Imamoglu, and J.P.Marangos 2005 *Rev. Mod. Phys.* **77** 633.
- [34] J. Kästel, M. Fleischhauer,S. F. Yelin and R. L. Walsworth 2007 *Phys.Rev.Lett.* **99** 073602.
- [35] N.A.Proite,B.E.Unks,J.T.Green,D.D.Yavuz 2008 *Phys.Rev.Lett.* **101** 14701.
- [36] J.D.Jackson 2001 *Classical Electrodynamics(3rd)*,NewYork:John Wiley & Sons, Chap.4, p.159-162.
- [37] D.M.Cook 1975 *The Theory of the Electromagnetic Field*,New Jersey: Prentice-Hall,Inc.,Chap. 11.
- [38] J.W. Shin,J.T. Shen,S.H.Fan 2009 *Phys.Rev.Lett.* **102** 093903.